Polytopic Linear Modeling of nonlinear mechanical systems

Document status and date:
Published: 01/01/1999

Document Version:
Publisher's PDF, also known as Version of Record (includes final page, issue and volume numbers)

Please check the document version of this publication:

• A submitted manuscript is the version of the article upon submission and before peer-review. There can be important differences between the submitted version and the official published version of record. People interested in the research are advised to contact the author for the final version of the publication, or visit the DOI to the publisher's website.
• The final author version and the galley proof are versions of the publication after peer review.
• The final published version features the final layout of the paper including the volume, issue and page numbers.

Link to publication

Download date: 04. Oct. 2023

Polytopic Linear Modeling of nonlinear mechanical systems:

A data based P.L.M. generating method

Rick Tebbens

Report No. 99.030

Eindhoven, 15 Novenber 1999

Coaches: Ir. G.Z. Angelis
                Dr. ir. M.J.G. van de Molengraft

Summary

Consider the nonlinear model:

$$\Sigma : \dot{x} = f(x,u)$$

The idea is to approximate Σ from data, by a Polytopic Linear Model (PLM) with a required accuracy ε. With the knowledge of the PLM it is possible to design a controller in a structural manner.

The local linear models are derived with two different methods:

- A method that evaluates the equation error: the Least Squares Method.
- A method that evaluates the output error: the Kalman Filter Method.

As each method uses its own criterion regarding the accuracy ε of the approximation, different results are expected: the Kalman filter method will produce a PLM that is capable of predicting trajectories on the long term whereas the least squares method will produce a PLM that is able to predict fast dynamics.

In order to get operating regimes that satisfy the prescribed accuracy ε, a procedure 'segregate' has been formulated. This procedure approximates Σ at first with only one linear model. If this approximation does not satisfy the required accuracy the operating space Z will be divided in into smaller operating regimes Z_i until the required accuracy is reached.

Both procedures are tested on data generated by a robot arm. The Kalman filter method proved to be superior to the least squares method, especially when the generated data contains noise.

Contents

1. Introduction

Consider the nonlinear model:

$$\Sigma : \dot{x} = f(\psi)$$

with information vector $\psi \in \Psi = \chi \times U$, state $x \in \chi \subset \Re^n$, input $u \in U \subset \Re^m$ and output $y \in Y \subset \Re^p$.

The idea is to approximate Σ by a Polytopic Linear Model (PLM) with a required accuracy ε. With the knowledge of the PLM it is possible to design a controller in a structural manner. The PLM is described by

$$\Pi : \dot{x} = \sum_{i=1}^{N_m} w_i(z)\{A_i x + B_i u + b_i\} = M(\psi)$$

A PLM is also a nonlinear model, build from a number (N_m) of local non-homogeneous linear models which are characterized by the triples (A_i, B_i, b_i), $i \in \{1..N_m\}$. Each linear model characterizes the quantitative behaviour of Σ in an operating regime Z_i. Each operating regime is described by a membership function $w_i(z)$; typically $w_i(z) \approx 1$ if (A_i, B_i, a_i) characterizes Σ and $w_i(z)=0$ elsewhere. The union of all operating regimes Z_i describes a compact operating space, $Z = \cup_{i=1}^{N_m} Z_i$. The accuracy ε of the approximation is initially defined as $\|\Sigma(\psi) - M(\psi)\|_2 \leq \varepsilon, \forall \psi \in \Psi$ with $\|...\|_2$ the Euclidean vector norm. $\Sigma(\psi)$ and $M(\psi)$ mean the right hand-side of the ordinary differential equations by which Σ respectively M are discribed Later on a different criterion will be evaluated.

In order to get operating regimes that satisfy the precribed accuracy ε, a procedure 'segregate' has been formulated. This procedure approximates Σ at first with only one linear model. If this approximation does not satisfy the required accuracy the operating space Z will be divided into smaller operating regimes Z_i until the required accuracy is reached (see figure 1).
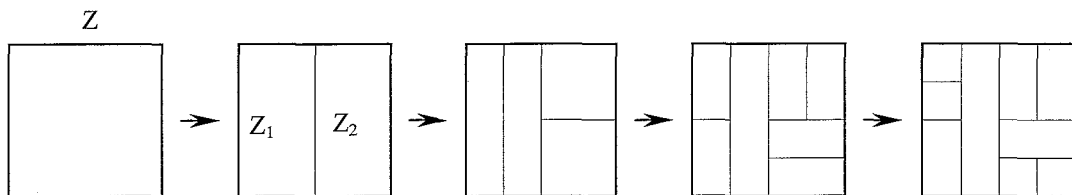
Figure 1: The segregation procedure

The fundamentals of this procedure can be found in the thesis of Joris Verstraete (Polytopic Linear Modeling of Nonlinear Mechanical Systems [1]).

2. The model

Throughout this report the two methods will be evaluated in the light of the model of the rotating arm. This will be useful for later measurements on the real rotating arm in the laboratory.

At first a simple non-linear model of a rotating arm has been made (the pendulum itself will not be considered):
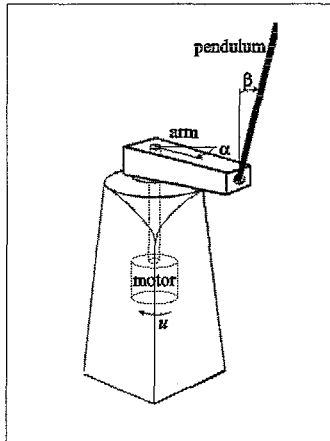
Figure 2: The rotating arm.

$$\Sigma : \begin{cases} \dot{x}_1 = f_1(\psi) = x_2 \\ \dot{x}_2 = f_2(\psi) = J^{-1} \cdot \left(k \cdot u - B_1 \cdot \dot{x}_2 - B_2 \dot{x}_2^{\,2} sign(\dot{x}_2) + f \cdot \frac{2}{\pi} \cdot a \tan(100 \cdot \dot{x}_2) \right) \end{cases}$$

$$\begin{bmatrix} x_1 \\ x_2 \end{bmatrix} = \begin{bmatrix} \alpha \\ \dot{\alpha} \end{bmatrix} ; \ \psi = \begin{bmatrix} x_1 \\ x_2 \\ u \end{bmatrix} \ \text{with} \ \psi \in \Psi .$$

This model has already proven its validity in former simulations.

In the rest of this report it will be assumed that $f_2(\psi)$ is always linear in u therefore, the information space Ψ can be projected onto a lower dimensional operating space Z:

$$Z = \begin{bmatrix} x_1 \\ x_2 \end{bmatrix} .$$

Further reduction of the operating space is impossible because the intention of this report is to approximate an *unknown* system with a desired accuracy. So, there is no information on the non-linearity of the system.
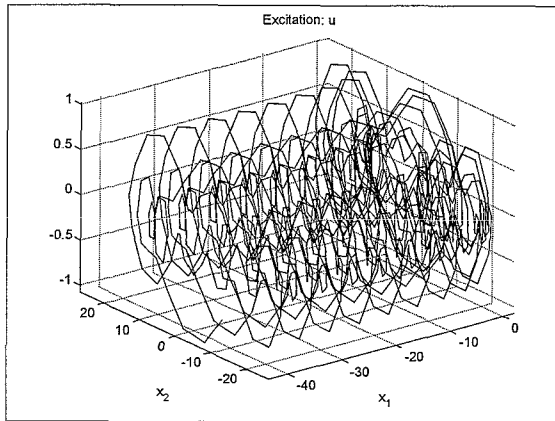
Figure 3a: The excitation u and corresponding trajectory (= information space Ψ).
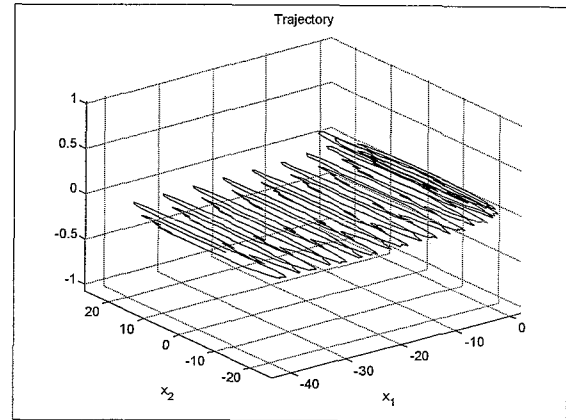
Figure 3b: The trajectory (=operating space Z).

Subsequently the model has been used for several simulations. The excitation u has to be chosen very carefully, as it will determine the trajectory and therefore the boundaries of the information space (Ψ). Further, u should be persistently exciting i.e. a broad spectrum of frequencies and amplitudes should be represented in the signal u in order to 'kick' the sytem everywhere in the information space. The simulation provides a column containing the measurements m_1 and m_2 of α and $\dot{\alpha}$ respectively over a certain time-span at fixed time intervals in response of the presented excitation. Figure 3a and 3b present an example of a three dimensional information space Ψ projected onto a two-dimensional operating space Z.

3. The segregation procedure

The segregation procedure can easily be explained by considering a two-dimensional operating space (position and velocity on the rotating arm). At first, the total operating space is evaluated. After establishing a linear model, the maximum error over this area is determined. The error should always be indicative of the difference between the linear model and the real non-linear model. If the error exceeds the prescribed accuracy then the operating space should be divided into two equal parts; the first division will take place upon the first state (x_1) the second division will take place upon the second state (x_2). The dimension of the operating space determines the number of divisions: a n-dimensional operating space Z will have n-possible decompositions. Depending upon which division gives the best accuracy, one of the two decompositions will be chosen. The criterion used here:
$\min(e(Z_1)+e(Z_2), e(Z_3)+e(Z_4))$.
The created sub-spaces Z_i will contain that part of the trajectory that lies in the chosen division. This sub-space can now be expanded with the corresponding u to determine a new set of local linear models and can, if necessary, again be divided into two equal parts and so on. This procedure is repeated until the desired accuracy is reached.

There are some limitations:
- If the divisions give no further improvement regarding the error, in comparison to the former error of the undivided space, the division for that region is stopped.
- When there aren't enough measurements left to divide, the procedure is stopped (this means that either the chosen accuracy is too high or the number of measurements is too small).
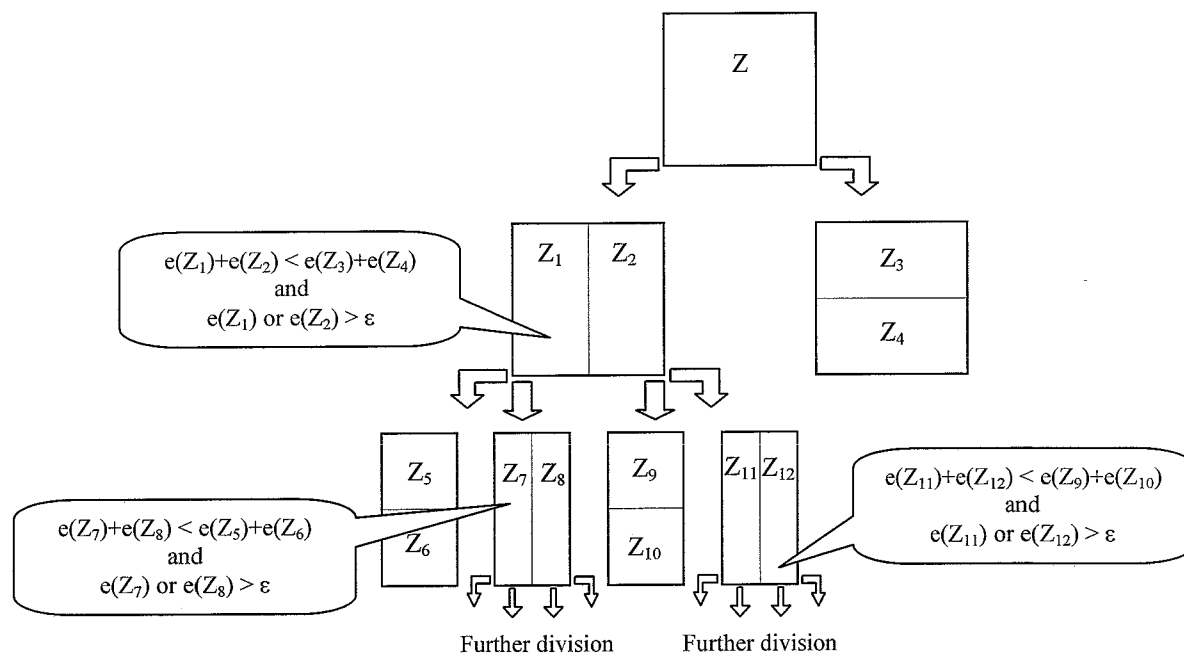

Figure 4: The segregation procedure

Figure 5 gives a graphic representation of the segregation procedure.

In the segregation procedure it is assumed that the total state is available but on the real rotating arm only x_1 (the position of the arm) is observed which means that x_2 has to be reconstructed. Because there is little or no information about the system available, x_2 is reconstructed by taking the time derivative of x_1 instead of using a Kalman filter. The state is reconstructed as follows:

$$x_2(k) = \frac{\dfrac{x_1(k) - x_1(k-1)}{dt} + \dfrac{x_1(k+1) - x_1(k)}{dt}}{2}$$

The segregation procedure was implemented in MATLAB 5.2. Below, a description of the relevant script-files and their variables will be given.

− A file named 'metingen.m' contains all the measurements namely:

   − The (reconstructed) state ($\underline{x}$).

   − The time derivative of the state ($\underline{\dot{x}}$). This is only used by The Least Squares Method (chapter 4).

   − The excitation (u).

   − The discrete time instants of measurement (t).

   These four variables have to be combined in a single matrix 'metingen':

$$metingen = \begin{bmatrix} \vdots & \vdots & \vdots & \vdots & \vdots & \vdots & \vdots & \vdots \\ u & x_1 & \cdots & x_n & \dot{x}_1 & \cdots & \dot{x}_n & t \\ \vdots & \vdots & \vdots & \vdots & \vdots & \vdots & \vdots & \vdots \end{bmatrix} \left.\right\} number \ of \ measurements, \ n \ states$$

− The accuracy (ε). The accuracy of The Least Squares Method can be found in the file 'segregate.m'. The accuracy of The Kalman Filter Method can be found in the file 'get_values.m'. This file also contains other specific parameters.

The procedure produces the following variables:

− A matrix 'S' which contains all the identified linear models of the various areas. The matrix 'S' is also stored in a file named 'file_s.mat'.

$$S = \begin{bmatrix} A^1_{11} & \cdots & A^1_{1n} & B^1_1 & b^1_1 \\ \vdots & \ddots & \vdots & \vdots & \vdots \\ A^1_{n1} & \cdots & A^1_{nn} & B^1_n & b^1_n \\ \vdots & \vdots & \vdots & \vdots & \vdots \\ A^k_{11} & \cdots & A^k_{1n} & B^k_1 & b^k_1 \\ \vdots & \ddots & \vdots & \vdots & \vdots \\ A^k_{n1} & \cdots & A^k_{nn} & B^k_n & b^k_n \end{bmatrix} \begin{matrix} \left.\right\} Area \ 1 \\ \\ \\ \left.\right\} Area \ k \end{matrix} \quad , \ (n \ states)$$

− A matrix 'final_state' which contains the boundary conditions for x of the various areas. The matrix 'final_state' is also stored in a file named 'file_st.mat'.

$$final\_state = \begin{bmatrix} x^1_1(\min) & x^1_1(\max) \\ \vdots & \vdots \\ x^1_n(\min) & x^1_n(\max) \\ \vdots & \vdots \\ x^k_1(\min) & x^1_1(\max) \\ \vdots & \vdots \\ x^k_n(\min) & x^k_n(\max) \end{bmatrix} \begin{matrix} \left.\right\} Area \ 1 \\ \\ \\ \left.\right\} Area \ k \end{matrix} \quad , \ (n \ states)$$

− A column 'final_e' which contains the accuracy of the various areas. The matrix 'final_e' is also stored in a file named 'file_e.mat'.

```
                          ┌─────────────┐
                          │    Start    │
                          └──────┬──────┘
                                 │
                                 ▼
      ┌──────────────────┐           ┌──────────────────────┐
      │ Determine error in│◄─────────►│ Function: 'kl_kw.m'  │
      │ whole state-space │           │ or 'Kalman_2.m'      │
      └────────┬─────────┘           └──────────────────────┘
               │
               ▼
      ┌──────────────────┐
      │ Update 'info':   │
      │ 'te_delen_x' = whole│
      │   state-space    │
      └────────┬─────────┘
               │
               ▼
             ╱─────╲                            Yes
            ╱ Error  ╲──────────────────────────────────────────┐
            ╲  < ε ?  ╱                                          │
             ╲─────╱                                            │
               │                                                │
               ▼                                                │
      ┌──────────────────┐                                      │
      │ Column 'info' gives│                                    │
      │ which part of     │                                    │
      │ 'te_delen_x' should│                                   │
      │   be divided      │                                    │
      └────────┬─────────┘                                     │
               │                                               │
               ▼                                               │
      ┌──────────────────┐      ┌──────────────────┐           │
      │ Divide selected part│◄──►│ Function:'deel.m'│           │
      │ from 'te_delen_x' in│    └──────────────────┘           │
      │ two optimal equal  │                                   │
      │   sub-spaces.      │                                   │
      └──┬────────────┬────┘                                   │
         │            │                                        │
         ▼            ▼                                        │
    ╱─────╲        ╱─────╲                                     │
Yes╱ Error  ╲  No ╱ Error  ╲Yes                                │
◄──╲ sub-   ╱────╲ sub-    ╱──┐                                │
   ╲space 2<ε?   ╲space 1<ε?  │                                │
    ╲───╱          ╲───╱      │                                │
     │      │         │       │                                │
     ▼      ▼         ▼       ▼                                │
```

Put sub-space in column: 'final_state' | Put sub-space in column: 'te_delen_x' | Put sub-space in column: 'final_state'

Put local linear model in column: 'S' | Update matrix 'info1' with new indices sub-space | Put local linear model in column: 'S'

All sub-spaces have been evaluated?   No

Reset and update 'info' with index of 'index1'

Reset 'info1'

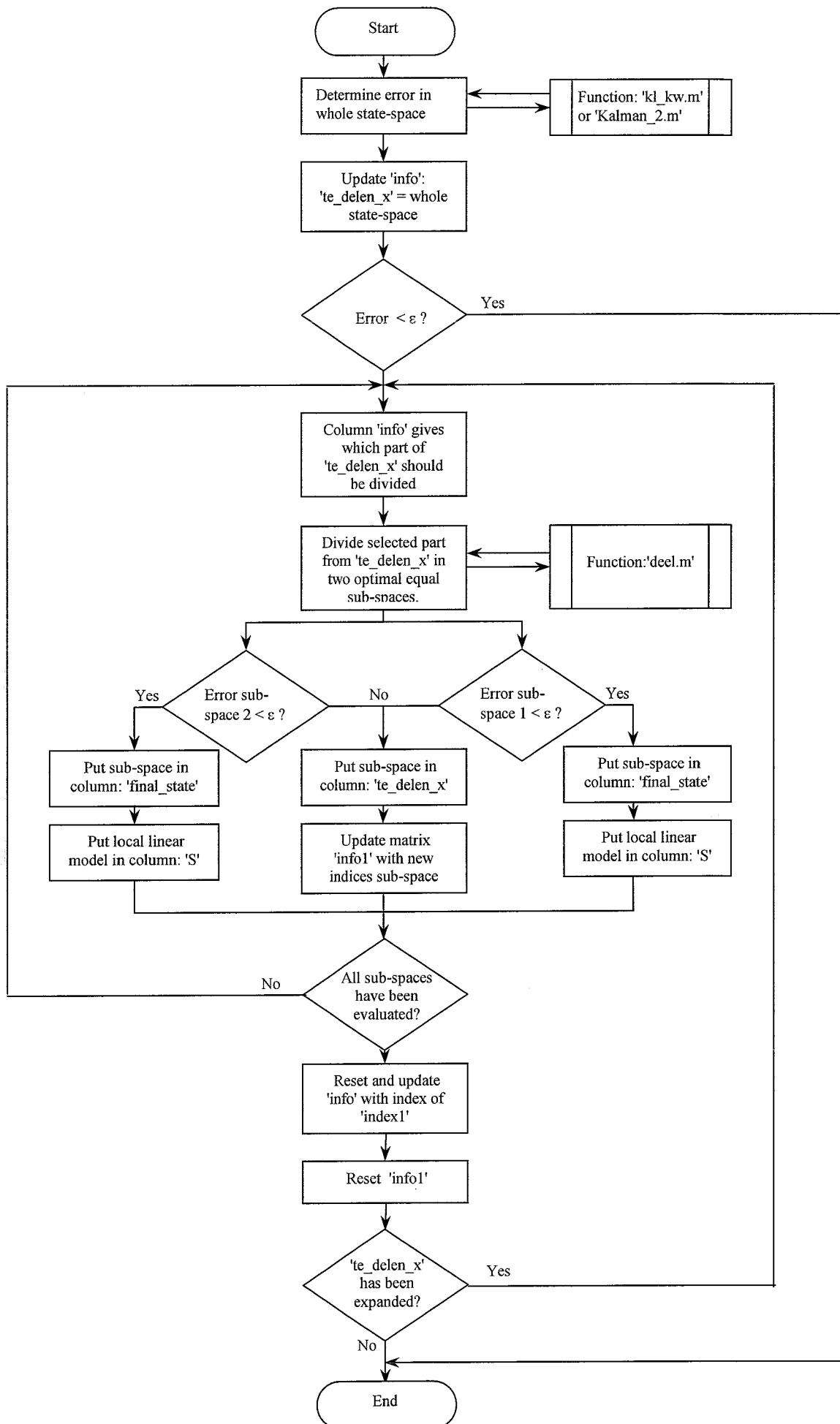'te_delen_x' has been expanded?   Yes

No

End

Figure 5: A graphic representation of the procedure 'segregate'.

7

4. Least squares method

After having discussed the segregation procedure, the next question is how to determine the local linear models. The first method is analogous to the method presented in the thesis of Joris Verstraete (*Polytopic Linear Modeling of Nonlinear Mechanical Systems* [1]) i.e. the same criterium ε will be evaluated.

The local linear models are of the following form:

$$\Pi_i : \begin{bmatrix} \dot{x}_1 \\ \dot{x}_2 \end{bmatrix} = \begin{bmatrix} A_i(1,1) & A_i(1,2) \\ A_i(2,1) & A_i(2,2) \end{bmatrix} \cdot \begin{bmatrix} x_1 \\ x_2 \end{bmatrix} + \begin{bmatrix} B_i(1) \\ B_i(2) \end{bmatrix} \cdot u + \begin{bmatrix} b_i(1) \\ b_i(2) \end{bmatrix}$$

The number of the evaluated area is given by the index i.

Π_i is determined by establishing a minimal equation error by means of the least square estimator below:

$$\min_\theta \sum \left(\dot{\hat{x}}_i - \Pi_i(\theta, \hat{x}, u) \right)^2 ; \quad \theta = \begin{bmatrix} A_i(1,1) & A_i(1,2) & A_i(2,1) & A_i(2,2) & B_i(1) & B_i(2) & b_i(1) & b_i(2) \end{bmatrix}^T$$

The non-linearity is approximated by evaluating the error: $e = \left\| \max\left(\dot{\hat{x}}_i - \Pi_i(\theta, \hat{x}, u) \right) \right\|_2$.

It is emphasized that the measurements in the evaluated area will, in general, not be a continuous time series, but a collection of fragments from the data.

4.1. Validation

Thereupon, three simulations have been executed to validate the above procedure (the desired accuracy ε is set to 2).

In the first simulation the model is reduced to a linear model (Coulomb-friction is neglected):

$$\Sigma : \begin{cases} \dot{x}_1 = f_1(\psi) = x_2 \\ \dot{x}_2 = f_2(\psi) = J^{-1} \cdot \left(k \cdot u - B_1 \cdot \dot{x}_2 \right) \end{cases} \Rightarrow \dot{\underline{x}} = A \cdot \underline{x} + B \cdot u \approx \begin{bmatrix} 0 & 1 \\ 0 & -3.7143 \end{bmatrix} \cdot \underline{x} + \begin{bmatrix} 0 \\ 594.2797 \end{bmatrix} \cdot u$$

The operating space that follows from the simulation with this model can be approximated with sufficient accuracy with only one linear model. Figure 6 shows that the error does not exceed $2.5 \cdot 10^{-8}$.
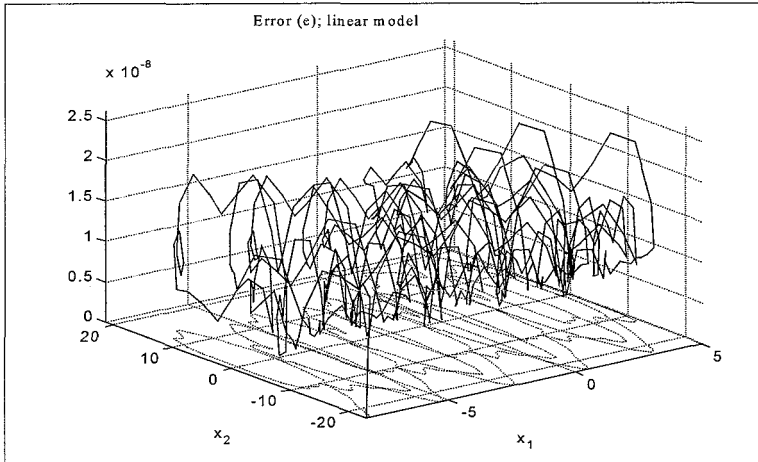

Figure 6: The error at the different points of the trajectory.

The least square estimator gives the following results:

$$A_1 = \begin{bmatrix} 0.0000 & 1.0000 \\ 0.0000 & -3.7142 \end{bmatrix}, \ B_1 = \begin{bmatrix} 0.0000 \\ 594.2797 \end{bmatrix}, \ b_1 = 1 \cdot 10^{-9} \cdot \begin{bmatrix} -0.0074 \\ -0.8373 \end{bmatrix}$$

Next, the model is expanded with one local non-linearity in the x_2 direction namely a "steep" arctangent function. The arctangent function is supposed to account for Coulomb-friction.

$$\Sigma: \begin{cases} \dot{x}_1 = f_1(\psi) = x_2 \\ \dot{x}_2 = f_2(\psi) = J^{-1} \cdot \left(k \cdot u - B_1 \cdot x_2 + f \cdot \dfrac{2}{\pi} \cdot a \tan(100 \cdot x_2) \right) \end{cases}$$

Segregation of the operation space, which follows from simulations with this model, leads to the results that are presented in figure 7.
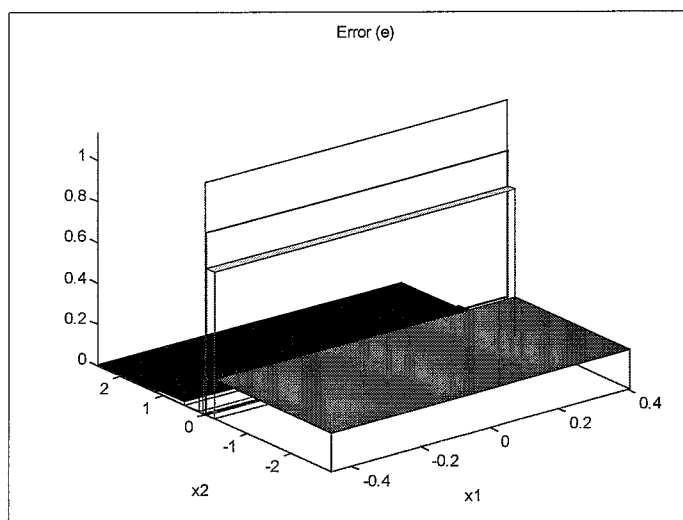

Figure 7: The segregation of the operating space and corresponding error.

It can be seen that around $x_2 = 0$, this is where the non-linearity is located, the operating space is divided in smaller sub-spaces. In figure 8 the results of a simulation with the reconstructed model are presented. There is only little difference between the reconstructed model and the original model so these results are very satisfactory.
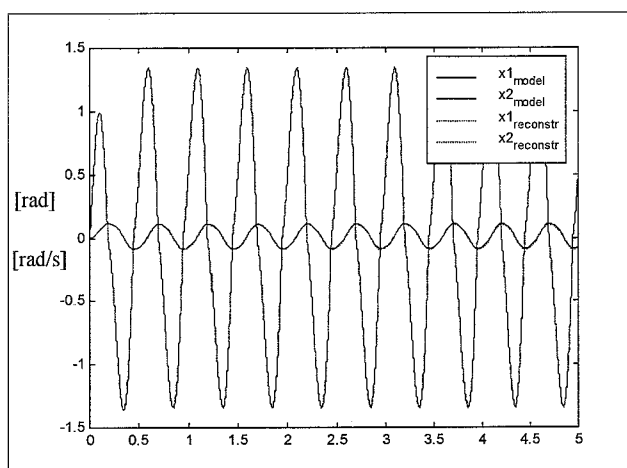

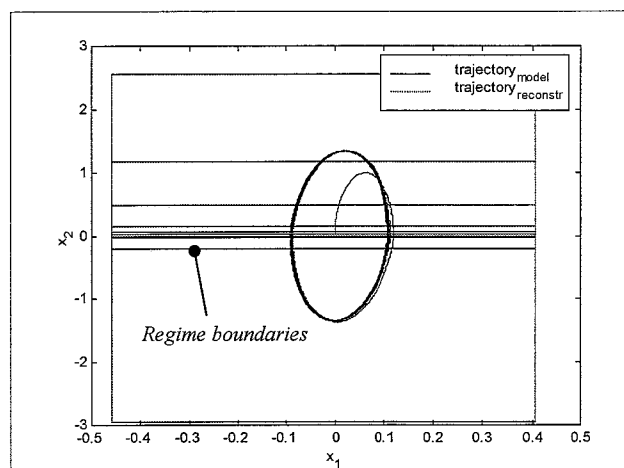*Figure 9a: difference between the reconstructed and the original model.*

Figure 9b: difference between the reconstructed and the original model (state space representation).

9

Finally the model is changed into the equation below, that has only one global non-linearity in the x_2 direction (this non-linearity is apart from $x_2=0$, constant):

$$\Sigma : \begin{cases} \dot{x}_1 = f_1(\psi) = x_2 \\ \dot{x}_2 = f_2(\psi) = J^{-1} \cdot \left(k \cdot u - B_1 \cdot x_2 - B_2 x_2^{\,2} sign(x_2) \right) \end{cases}$$

The results of segregation of the latter are presented in figure 8. Since the non-linearity can be associated with the second order Taylor remander, which in this case is constant, the operating space will be divided in equally sized sub-spaces.
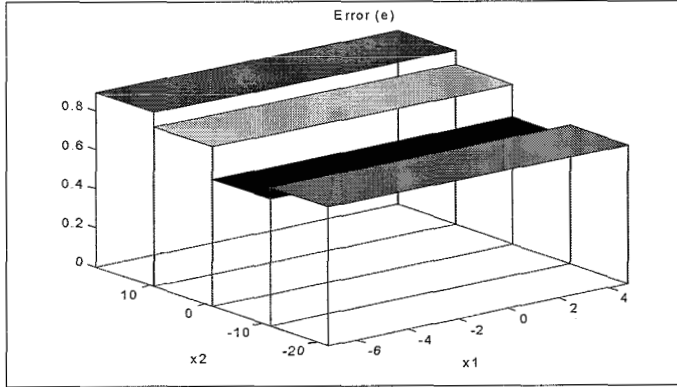

Figure 9: The segregation of the operating space and corresponding error.

10

5. Kalman filter method

The Kalman filter implementation of the segregation method shows several differences with the previous least squares approach:

  — Instead of the least squares estimator, now a Kalman filter has been used to estimate the extended state. It is assumed that the linear approximation of the system is of the following form:

$$\Pi_i : \begin{bmatrix} \dot{x}_1 \\ \dot{x}_2 \end{bmatrix} = \begin{bmatrix} 0 & 1 \\ A_i(2,1) & A_i(2,2) \end{bmatrix} \cdot \underline{x} + \begin{bmatrix} 0 \\ B_i(2) \end{bmatrix} \cdot u + \begin{bmatrix} 0 \\ b_i(2) \end{bmatrix}$$

The state will be extended to:

$$\underline{x} = \begin{bmatrix} x_1 & x_2 & A(2,1) & A(2,2) & B(2) & b(2) \end{bmatrix}^T .$$

This results in a (non-linear) system with an extended state:

$$\dot{\underline{x}} = g(x,u) = \begin{bmatrix} 0 \cdot x_1 + 1 \cdot x_2 + 0 \cdot u + 0 \\ x_3 \cdot x_1 + x_4 \cdot x_2 + x_5 \cdot u + x_6 \\ 0 \\ 0 \\ 0 \\ 0 \end{bmatrix} = \begin{bmatrix} x_2 \\ x_3 \cdot x_1 + x_4 \cdot x_2 + x_5 \cdot u + x_6 \\ 0 \\ 0 \\ 0 \\ 0 \end{bmatrix}$$

The Kalman filter design involves the choice of a number of tuning parameters:

- The noise intensity. Matrix Q and R representing system and measurement uncertainty respectively.
- P_0 representing the initial state variance.

  — In the previous method, Π_i is determined by the least square estimator: $\min_\theta \sum \left(\hat{\underline{x}}_i - \Pi_i(\theta, \underline{x}) \right)^2$. Because the

reconstructed state ($\hat{\underline{x}}$) will always consist partially of noise, an estimate of $\dot{\hat{x}}$ obtained by numerical differentation of $\hat{x}$ will not be very accurate since the noise will be amplified. The non-linearity of the estimated linear model with the new procedure is evaluated by regarding the new error e. The non-linearity is given by the new definition of the error (= output error):

$$e = \frac{1}{t_e - t_0} \cdot \int_{t=t_0}^{t_e} \left(r^T \cdot Q \cdot r + s^T \cdot R \cdot s \right) \cdot dt$$

r is the innovation: $r = K \cdot (m - H \cdot \hat{x})$.

s is the difference between the measurement and the reconstructed state: $s = m - H \cdot \hat{x}$.

Apart from the fact that noise will be amplified in the least squares method, the second method will estimate polytopic models that are more capable of reproducing the estimated state in the long term.

The error is determined by a second state reconstruction (i.e. only the position and the velocity are estimated and all other parameters are fixed) with the model that was estimated with the first Extended Kalman filter. In this way the total region Z_i will be evaluated with the best possible estimation of the parameters A(2,1), A(2,2), B(2) and b(2) in order to establish the corresponding error.

The implementation of this method produced a considerable difficulty: the path of the chosen trajectory is in this case of great significance. When the state-space is divided in two sub-spaces, the trajectory will also be divided into two parts. These leads to discontinuities in the state-space, see figure 10. Because the Kalman filter intends to minimize the difference between the estimated and the real state, the number of discontinuities will determine the degree in which the filter is able to reconstruct the divided trajectory. This means that a division, which leads to a lot of disconnected data fragments, produces a large error. Therefore the Kalman filter first estimates the extended state from the first data fragment. Next, the Kalman filter estimates the extended state from the second data fragment but this time the filter is initialized with the estimated parameters of the former augmented state. The initial value of the corresponding state variance will also be taken from the former estimation. This process is repeated for all the other data fragments.
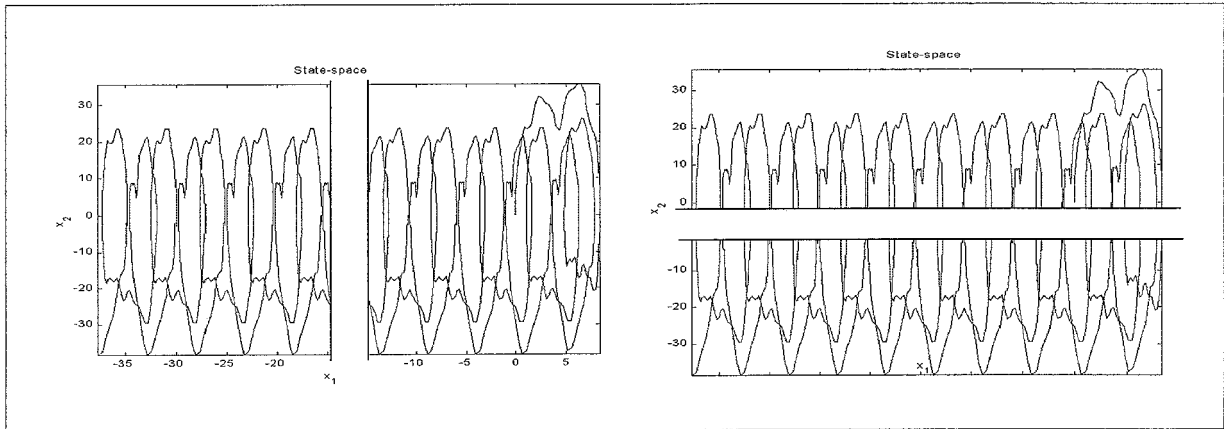

Figure 10: Discontinuities in the operating space.

Figure 11 shows the implementation of this re-initialize procedure. In this case the operating space is divided in two regions: $x_2 > 0$ and $x_2 < 0$. The second region is used to estimate the various parameters. It can be seen that in spite of the discontinuities in the trajectory, the Kalman filter is still able to realize convergence of the parameters.
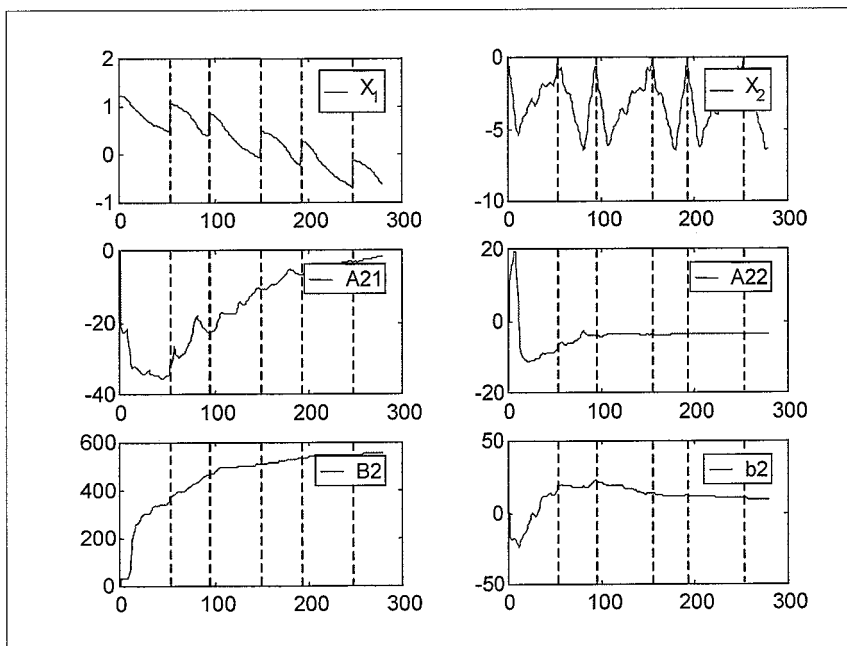

Figure 11: Estimation of the parameters from a discontinuous data set.

12

5.1. Validation

In the first experiment the model is again reduced to a linear model (the chosen excitation is a chirp signal):

$$\Sigma : \begin{cases} \dot{x}_1 = f_1(\psi) = x_2 \\ \dot{x}_2 = f_2(\psi) = J^{-1} \cdot (k \cdot u - B_1 \cdot x_2) \end{cases} \Rightarrow \underline{\dot{x}} = A \cdot \underline{x} + B \cdot u \approx \begin{bmatrix} 0 & 1 \\ 0 & -3.7143 \end{bmatrix} \cdot \underline{x} + \begin{bmatrix} 0 \\ 594.2797 \end{bmatrix} \cdot u$$

The Kalman Filter method only needed one model to reach an accuracy of $\varepsilon = 0.0042$. The following model is estimated:

$$A_1 = \begin{bmatrix} 0 & 1 \\ -0.0699 & -3.6596 \end{bmatrix}, \ B_1 = \begin{bmatrix} 0 \\ 587.6379 \end{bmatrix}, \ b_1 = \begin{bmatrix} 0 \\ -0.0289 \end{bmatrix}$$

Next, the non-linear arctangent function is added to the previous linear model:

$$\Sigma : \begin{cases} \dot{x}_1 = f_1(\psi) = x_2 \\ \dot{x}_2 = f_2(\psi) = J^{-1} \cdot \left(k \cdot u - B_1 \cdot \dot{x}_2 + f \cdot \dfrac{2}{\pi} \cdot a\tan(100 \cdot \dot{x}_2) \right) \end{cases}$$

Segregation of the operation space, which follows from simulations with this model, provides the results that are presented in figure 12.
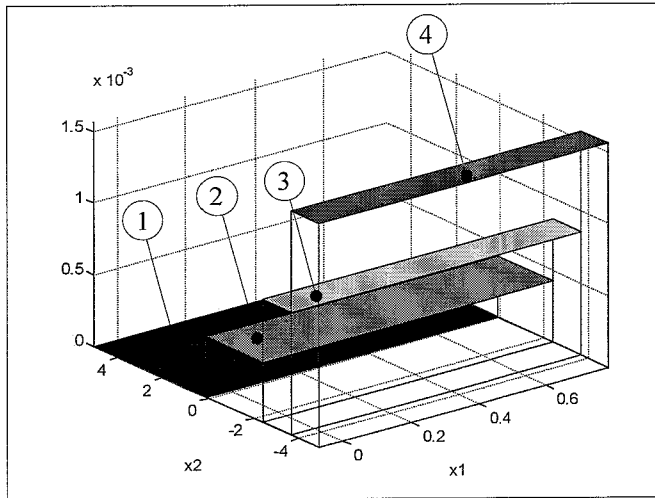

Figure 12: The segregation of the operating space and the corresponding error

The estimated linear models of the areas 1, 2, 3 and 4 (figure 10) are:

$$A_1 = \begin{bmatrix} 0 & 1 \\ -2.9674 & -3.9745 \end{bmatrix}, \ B_1 = \begin{bmatrix} 0 \\ 589.8500 \end{bmatrix}, \ b_1 = \begin{bmatrix} 0 \\ -8.5498 \end{bmatrix}$$

$$A_2 = \begin{bmatrix} 0 & 1 \\ 1.5378 & -6.5386 \end{bmatrix}, \ B_2 = \begin{bmatrix} 0 \\ 588.3895 \end{bmatrix}, \ b_2 = \begin{bmatrix} 0 \\ 5.4557 \end{bmatrix}$$

$$A_3 = \begin{bmatrix} 0 & 1 \\ -8.1343 & -5.1281 \end{bmatrix}, \ B_3 = \begin{bmatrix} 0 \\ 574.9535 \end{bmatrix}, \ b_3 = \begin{bmatrix} 0 \\ 9.9162 \end{bmatrix}$$

$$A_4 = \begin{bmatrix} 0 & 1 \\ -5.7703 & -5.2816 \end{bmatrix}, \ B_4 = \begin{bmatrix} 0 \\ 566.1097 \end{bmatrix}, \ b_4 = \begin{bmatrix} 0 \\ 4.9964 \end{bmatrix}$$

These results are not in accordance with what we expected on the basis of the original model. Figure 13 shows us the results of a simulation with the reconstructed model. In spite of the fact that the Kalman filter was unable to reconstruct the original parameters, the difference between the reconstructed model and the original model in the simulation is moderate.
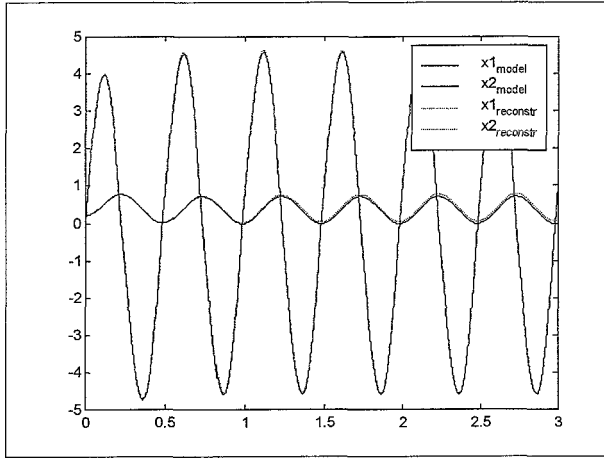

Figure 13a: difference between the reconstructed and the original model.
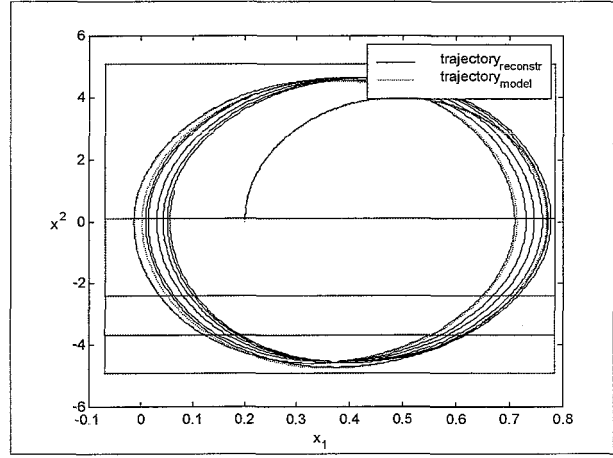

Figure 13b: difference between the reconstructed and the original model (state space representation).

Simulations with different excitations gave no significant improvement in the accuracy of the Polytopic model. A noteworthy fact is that an excitation of the following form enables the Kalman filter to give a better reconstruction of the parameters: choose a sine curve with a low frequency and a relative large amplitude then superimpose various sine curves with high frequencies and relative low amplitudes on the large sine curve.

14

6. Implementation on the robot arm

Finally, the two methods are implemented on the real robot arm and subsequently validated. Both methods use the same input signal (see figure 14) and therefore the boundaries of the operation space will be the same for the two methods. The input is the sum of a sine curve with a low frequency and relative large amplitude and four sine curves with high frequencies and relative low amplitudes. Next, this signal is multiplied with a part of a sine curve in order to decrease the total amplitude of the input signal. Figure 15 presents the operation space and the trajectory.
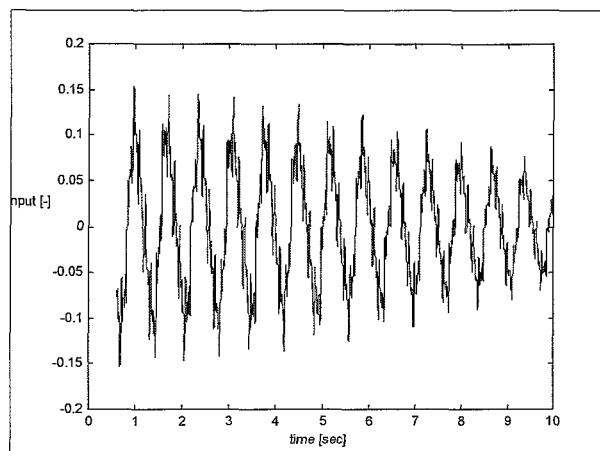
Figure 14: The input signal.
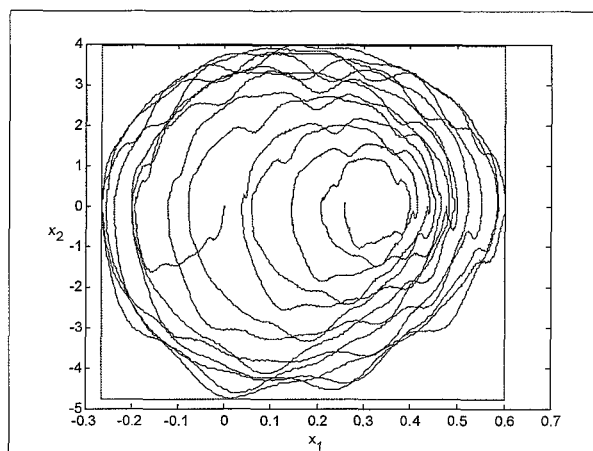
Figure 15: The boundaries of the operation space and the trajectory.

6.1. The least squares method

6.1.2. Determination of the Polytopic model

The trajectory from the robot arm and the time derivative is offered to the segregation procedure (the accuracy is set to 30). Figure 16 gives the various regions (Z_i) and the corresponding error. Appendix A gives the estimated parameters for the various regions.

Figure 16: The segregation of the operating space and the corresponding error

15

6.1.2 Validation

The established Polytopic model is now used for a validation. Figure 17a and b show the difference between a simulation with the Polytopic model and the data from the robot arm (figure 17a also show the regions Z_i). The excitation again was a combination of five sine curves with decreasing amplitude.
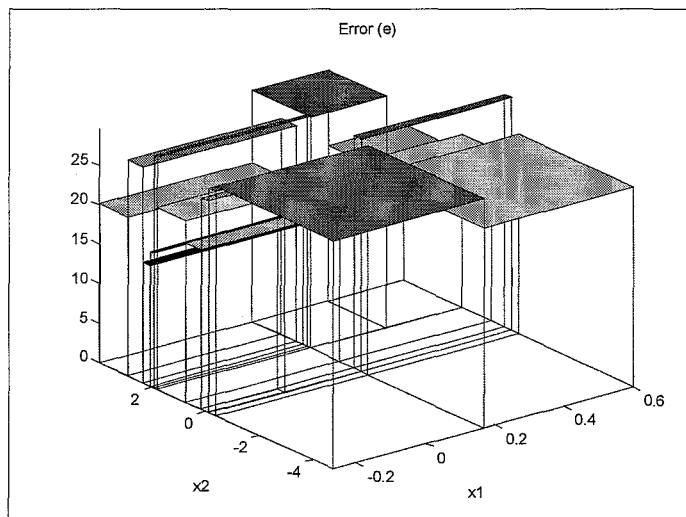

Figure 17a: difference between the reconstructed model and the real data (state space representation).
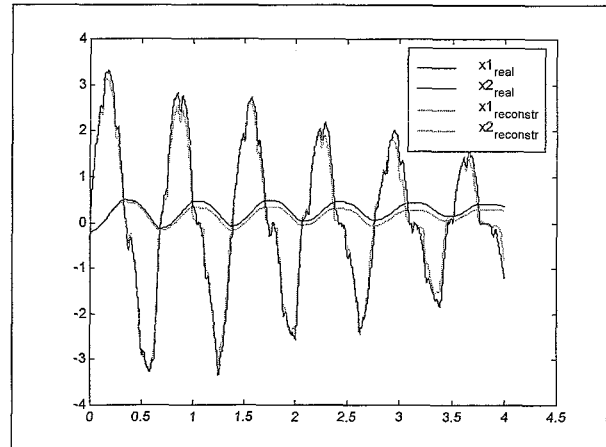
Figure 17b: difference between the reconstructed model and the real data.

6.2. The Kalman filter method

6.2.2. Determination of the Polytopic model

The same trajectory as used in 6.1.1. is offered to the segregation procedure (the accuracy is set to 0.01). Figure 18 gives the various regions (Z_i) and the corresponding error. It can be seen that the procedure wasn't able to reduce the error in region around zero. Appendix B gives the estimated parameters for the various regions.

Figure 18: The segregation of the operating space and the corresponding error

16

6.2.2 Validation

Again, the established Polytopic model is now used for a validation. Figure 19a and b show the difference between a simulation with the Polytopic model and the data from the robot arm (figure 19a also show the regions Z_i). The excitation was the same as used in 6.1.2.
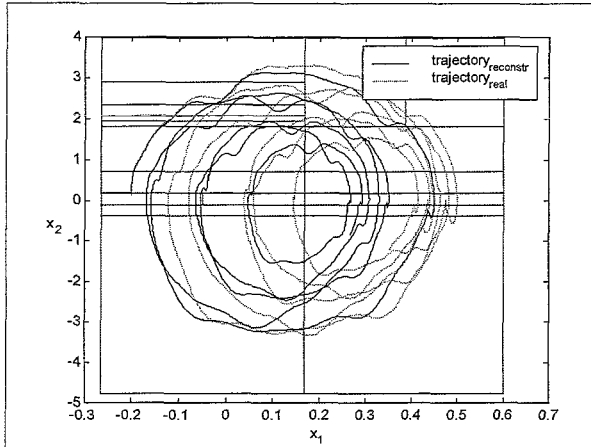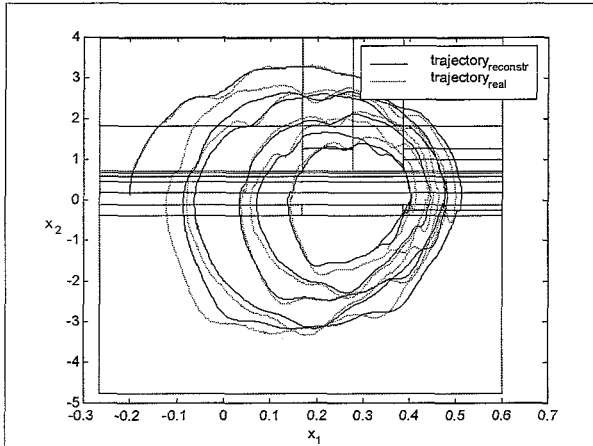

Figure 19a: difference between the reconstructed model and the real data (state space representation).

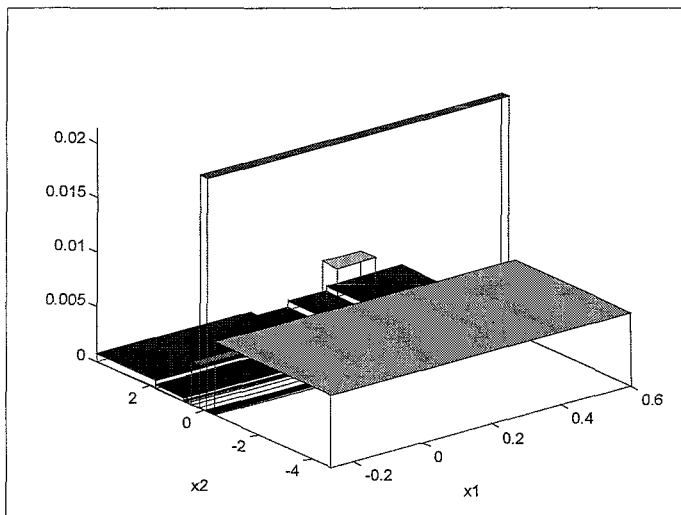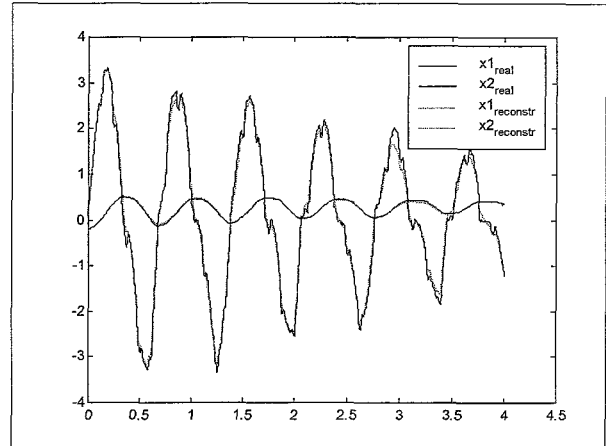Figure 19b: difference between the reconstructed model and the real data.

7. Conclusions and recommendations

Both the Kalman filter method and the least squares method are able to locate the non-linear Coulomb friction around $x_2 = 0$. The physical interpretation of the estimated parameters is not always possible. Especially in the regions where large non-linearities are expected, physical interpretation of the estimated parameters is impossible. In the regions where little non-linear behaviour is expected, the parameters give a insight in the value of friction for instance. Comparisons with former estimations of these parameters gave a fair resemblance (for instance area 1 of both methods, see appendix A-B).

From chapter 6 can be concluded that the Kalman filter method gives a better estimation of the Polytopic model when real data is used. This was in accordance with was predicted in chapter 5: the least squares method uses disturbed data by using the first and the second time derivative of the position. Furthermore, the Kalman filter takes noise on the data into account and instead of minimizing the equation error, it minimizes the output error. The results of the Kalman filter method may even be improved by tuning the various Kalman filter parameters.

17

Appendix A: parameters least squares method

Area no.	State	Boundaries Min.	Max.	A_i		B_i	b_i
1	x_1	-0.2648	0.1683	0	1.0000	0	0
	x_2	-4.7517	-0.3829	-18.2856	-1.2218	481.5190	23.9648
2	x_1	0.1683	0.6013	0	1.0000	0	0
	x_2	-4.7517	-0.3829	14.4199	-4.1127	602.1557	14.2361
3	x_1	-0.2648	0.1683	0	1.0000	0	0
	x_2	0.7093	1.8015	11.6562	-0.8026	590.8541	-25.4660
4	x_1	-0.2648	0.1683	0	1.0000	0	0
	x_2	2.8937	3.9859	-19.3921	0.8431	573.9609	-32.9563
5	x_1	0.1683	0.6013	0	1.0000	0	0
	x_2	0.7093	1.8015	21.6698	-3.7276	627.6812	-25.8576
6	x_1	0.1683	0.3848	0	1.0000	0	0
	x_2	1.8015	3.9859	22.1751	-3.0580	609.7539	-25.1308
7	x_1	0.3848	0.6013	0	1.0000	0	0
	x_2	1.8015	3.9859	18.4341	-2.5407	649.2071	-28.4490
8	x_1	-0.2648	0.1683	0	1.0000	0	0
	x_2	0.1632	0.7093	18.0573	3.4350	597.5703	-26.8834
9	x_1	-0.2648	0.1683	0	1.0000	0	0
	x_2	2.3476	2.8937	-2.6536	-2.1289	580.4878	-23.5286
10	x_1	0.1683	0.6013	0	1.0000	0	0
	x_2	0.1632	0.7093	40.8529	-5.2896	666.3968	-33.4959
11	x_1	-0.2648	0.1683	0	1.0000	0	0
	x_2	-0.3829	-0.1098	4.3884	13.3992	369.0199	30.9914
12	x_1	-0.2648	0.1683	0	1.0000	0	0
	x_2	2.0746	2.3476	11.3317	5.9547	595.9408	-42.3285
13	x_1	0.1683	0.6013	0	1.0000	0	0
	x_2	-0.3829	-0.1098	31.8072	-2.3522	576.2903	6.0740
14	x_1	0.1683	0.6013	0	1.0000	0	0
	x_2	-0.1098	0.1632	-16.2024	-121.5153	267.1661	7.0177
15	x_1	-0.2648	-0.0483	0	1.0000	0	0
	x_2	-0.1098	0.1632	75.6074	-180.7296	687.2695	4.4644
16	x_1	-0.0483	0.1683	0	1.0000	0	0
	x_2	-0.1098	0.1632	-102.6026	-135.9894	256.9425	16.0896
17	x_1	-0.2648	0.1683	0	1.0000	0	0
	x_2	1.8015	1.9381	7.5859	26.3657	637.9353	-82.0566
18	x_1	-0.2648	0.1683	0	1.0000	0	0
	x_2	1.9381	2.0746	14.0793	12.8697	606.9565	-54.8950

Appendix B: parameters Kalman filter method

Area no.	State	Boundaries Min.	Max.	A_i		B_i	b_i
1	x_1	-0.2648	0.6013	0	1.0000	0	0
	x_2	-4.7517	-0.3829	-19.6306	-1.3388	474.5737	23.2652
2	x_1	-0.2648	0.1683	0	1.0000	0	0
	x_2	1.8015	3.9859	-24.3034	-3.3836	406.8478	-7.0187
3	x_1	-0.2648	0.1683	0	1.0000	0	0
	x_2	0.7093	1.8015	-15.0759	-2.9403	369.6105	-5.9302
4	x_1	0.3848	0.6013	0	1.0000	0	0
	x_2	1.8015	3.9859	-24.5307	-6.5162	374.8093	1.5409
5	x_1	-0.2648	0.6013	0	1.0000	0	0
	x_2	0.1632	0.4363	-14.6128	-10.8237	354.7136	-7.4879
6	x_1	0.1683	0.2765	0	1.0000	0	0
	x_2	1.8015	3.9859	-20.1223	-4.6237	373.2493	0.2875
7	x_1	0.2765	0.3848	0	1.0000	0	0
	x_2	1.8015	3.9859	-25.8769	-3.6231	366.1476	-2.5554
8	x_1	-0.2648	0.1683	0	1.0000	0	0
	x_2	-0.3829	-0.1098	-21.7033	-9.8994	337.5465	19.8181
9	x_1	-0.2648	0.6013	0	1.0000	0	0
	x_2	-0.1098	0.1632	-12.3130	-41.1949	230.6125	5.4659
10	x_1	-0.2648	0.6013	0	1.0000	0	0
	x_2	0.4363	0.5728	-22.4484	-10.9273	344.9230	-2.8270
11	x_1	0.2765	0.3848	0	1.0000	0	0
	x_2	0.7093	1.8015	-24.7331	-6.5735	351.7486	1.6675
12	x_1	0.3848	0.6013	0	1.0000	0	0
	x_2	1.2554	1.8015	-23.5115	-9.2669	359.3913	3.1342
13	x_1	0.1683	0.3848	0	1.0000	0	0
	x_2	-0.3829	-0.1098	-20.1245	-8.6843	338.2395	14.3558
14	x_1	-0.2648	0.6013	0	1.0000	0	0
	x_2	0.5728	0.6411	-16.7735	-11.4670	332.0291	-2.4134
15	x_1	-0.2648	0.6013	0	1.0000	0	0
	x_2	0.6411	0.7093	-20.3161	-10.9481	335.3594	-1.2280
16	x_1	0.1683	0.2765	0	1.0000	0	0
	x_2	0.7093	1.2554	-21.7525	-8.0048	337.8189	5.0920
17	x_1	0.1683	0.2765	0	1.0000	0	0
	x_2	1.2554	1.8015	-22.8421	-9.6383	337.5241	4.3743
18	x_1	0.3848	0.6013	0	1.0000	0	0
	x_2	0.7093	0.9824	-25.8317	-11.3728	345.0546	-1.3407
19	x_1	0.3848	0.6013	0	1.0000	0	0
	x_2	0.9824	1.2554	-23.5545	-10.6700	343.2975	1.1010
20	x_1	0.3848	0.6013	0	1.0000	0	0
	x_2	-0.3829	-0.2464	-17.1133	-9.0823	337.7909	13.8845
21	x_1	0.3848	0.6013	0	1.0000	0	0
	x_2	-0.2464	-0.1098	-15.7904	-8.4212	339.0424	16.1129

Bibliography

[1]   J. Verstraete. *Polytopic Linear Modeling of Nonlinear Mechanical Systems.* Internal report 99.019, 1999.

[2]   R.H.A. Hensen. *Extended Kalman Filter based System Identification Tool.* Internal report WFW 99.003, 1999.

[3]   A. Gelb. *Applied Optimal Estimation.* M.I.T. Press, 1996.